**THE EUROPEAN
PHYSICAL JOURNAL B**

Regular Article

Ferromagnetism of the repulsive atomic Fermi gas: three-body recombination and domain formation

Ilia Zintchenko[1], Lei Wang[1,2,a], and Matthias Troyer[1]

[1] Theoretische Physik, ETH Zurich, 8093 Zurich, Switzerland
[2] Beijing National Lab for Condensed Matter Physics and Institute of Physics, Chinese Academy of Sciences,
Beijing 100190, P.R. China

Abstract. The simplest model for itinerant ferromagnetism, the Stoner model, has so far eluded experimental observation in repulsive ultracold fermions due to rapid three-body recombination at large scattering lengths. Here we show that a ferromagnetic phase can be stabilised by imposing a moderate optical lattice. The reduced kinetic energy drop upon formation of a polarized phase in an optical lattice extends the ferromagnetic phase to smaller scattering lengths where three-body recombination is small enough to permit experimental detection of the phase. We also show, using time dependent density functional theory, that in such a setup ferromagnetic domains emerge rapidly from a paramagnetic initial state.

The ground-state of a repulsive gas of fermions with contact interaction was first predicted by Stoner [1] in 1933 to be ferromagnetic and a precise value for the critical interaction strength in a homogeneous system was recently obtained with diffusion Monte Carlo simulations [2–4]. While ultracold fermionic gases should provide a controlled environment to study this phenomenon, the instability of a strongly repulsive gas towards molecule formation has so far prevented experimental realization of this phase. Repulsive fermions on the positive side of the Feshbach resonance live on the meta-stable repulsive branch [5]. When three atoms, one with the opposite spin of the other two, come close to each other two atoms with opposite spin will form bosonic molecules and the other one carries the binding energy away. The rate of such process increases rapidly with scattering length. The lifetime of the gas is therefore largely governed by the interaction strength and the spatial overlap between the two spin species.

A recent experiment [6] presented evidence for a possible ferromagnetic state formed after rapid increase of the scattering length. The nature of this phase has, however, been questioned [7–9] as the peaks in kinetic energy, cloud size and loss rate observed in reference [6] are only indirect evidence for ferromagnetic domains [7], and it has been shown that molecule formation is dominant at large interaction strengths [8,9]. Several papers have proposed to reduce the recombination rate by using a polar molecular gas with dipole interactions and positive scattering range [10], narrower Feshbach resonances [8,9,11–13] and fermions with unequal mass [14,15]. Although these approaches might prove promising in experiments, as has

recently been shown in reference [16], they all change the microscopic physics of the Stoner model.

Here we suggest new strategies which achieve the same goal of stabilising the ferromagnetic phase, yet preserve the microscopic physics and thus pave the way towards experimental realization of Stoner ferromagnetism. Firstly, the lifetime of the system can be increased by reducing the overlap volume between polarized domains with different spins. This can be achieved using elongated traps with larger aspect ratios, but turns out to be insufficient to stabilise the phase by itself. A more effective way is to reduce the critical scattering length, at which ferromagnetism sets in, by imposing a shallow optical lattice [2,17]. The ferromagnetic transition is determined by a competition between the loss of kinetic energy and gain of interaction energy. Since the optical lattice reduces the kinetic energy scale, the ferromagnetic state is stabilised. A similar effect is found in flat band ferromagnetism [18–20]. On the other hand, ferromagnetism is not particularly favorable in an ordinary single band Hubbard model with finite interaction strength [21]. Reference [22] studied Hubbard model with infinite repulsive interaction, and discovered ferromagnetism in connection to the Nagaoka state [23]. However, in practice, the single band approximation of the Hubbard model may not hold in such strong interaction limit. In the shallow lattice case, an appropriate description is the multi band Hubbard model, where a substantial ferromagnetic region was discovered in reference [24].

To obtain quantitative results for the phase diagrams we use Kohn-Sham density functional theory [25,26] here the exchange-correlation energy is treated within a local spin density approximation (LSDA) which has been widely used for materials simulations and more
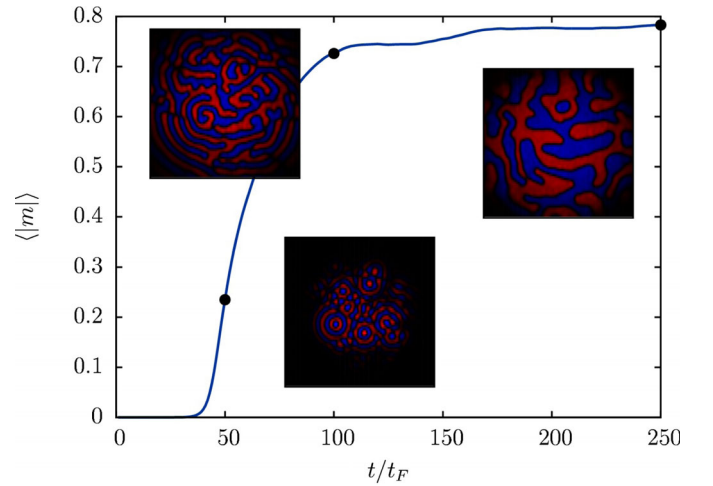
a e-mail: wanglei@iphy.ac.cn
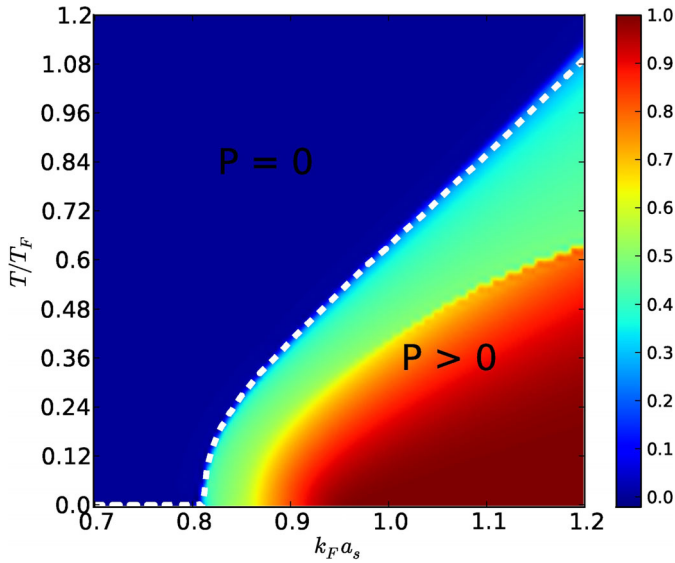
Fig. 1. Phase diagram of the homogeneous repulsive Fermi gas as a function of temperature T/T_F and interaction strength $k_F a_s$. The white dashed line indicates the paramagnet-ferromagnetic phase transition and the colour scale the polarization $P = (n_\uparrow - n_\downarrow)/(n_\uparrow + n_\downarrow)$.

**Fig. 2.** Total magnetisation $\langle |m| \rangle$ in pancake shaped harmonic confinement for $N = 440$. Starting from a paramagnetic phase the system evolves in the presence of thermal noise for $t \in [0; 250] t_F$. Topology of ferromagnetic domains at $t = \{50, 150, 250\} t_F$ is shown in the insets. As the gas remains unpolarised away from the center, the maximum magnetisation is ~ 0.8.

recently for ultracold atomic gases [17,27–29]. The LSDA exchange-correlation functional is obtained by solving a uniform system at zero temperature with diffusion Monte-Carlo [3,4], where interactions between fermionic atoms with opposite spin are modelled by a hard-sphere potential with scattering length a_s. We compute the spin density distribution and the three-body loss rate using Kohn-Sham orbitals.

Before discussing our proposal to stabilise the ferromagnetic phase we investigate whether thermal fluctuations, which can significantly affect of the stability of the ferromagnetic phase [30], might be responsible for the absence of a stable ferromagnetic phase in experiments. To quantify the effect of non-zero temperature we employ finite-temperature density functional theory with a zero temperature exchange-correlation correction [31–34]. The resulting phase diagram, presented in Figure 1, is in general agreement with previous results [35,36]. We observe almost full polarization in the currently experimentally accessible temperature regime $T \sim 0.25 T_F$ [8,13] and thermal fluctuations are thus not the dominant mechanism destabilising the ferromagnetic phase.

An equally important question is that of the time scale over which ferromagnetic domains form from an initially paramagnetic state [37], which should be within the capabilities of current experimental setups for the observation of ferromagnetic domains to remain plausible. We address this issue within the time-dependent Kohn-Sham formalism [38] ignoring the effect of three-body recombination. The system is evolved in pancake shaped harmonic confinement in the presence of thermal noise after a quench of the interaction strength $k_F^0 a_s$ to 1.2. Already after $t \sim 250 t_F$ ferromagnetic domains with a feature size $\sim 10 k_F^{-1}$ form (Fig. 2), which is within the resolution

currently achievable in the lab. The ferromagnetic phase is also significantly more stable with a total recombination rate reduced by a factor ~ 3 relative to the initial paramagnetic gas. In the experiment [8], more than half of the particles remain in the meta-stable repulsive branch after $250 t_F$. However, ferromagnetic domains were not observed indicating that three-body recombination has more significant effects beyond reducing the fraction of meta-stable fermions in the system.

We thus focus on three-body recombination and determine its effect on the stability of the ferromagnetic phase. The loss rate $\Gamma = -\partial_t N/N$ (N is the total number of particles in the system) is inversely proportional to the lifetime of the system and can be computed as [39]

$$\Gamma \sim a_s^3 \sum_\sigma \int d\boldsymbol{r} \int_{|\boldsymbol{r}'-\boldsymbol{r}|<a_s} d\boldsymbol{r}' \varepsilon_F(\boldsymbol{r}) g_{\bar{\sigma}\sigma\sigma}(\boldsymbol{r}, \boldsymbol{r}, \boldsymbol{r}') \quad (1)$$

where $\varepsilon_F(\boldsymbol{r}) = \hbar^2 (3\pi^2 (n_\uparrow + n_\downarrow))^{2/3}/2m$ is the local Fermi energy, $n_\sigma(\boldsymbol{r})$ is the local density of each spin, m the atom mass and $g_{\bar{\sigma}\sigma\sigma}(\boldsymbol{r}, \boldsymbol{r}, \boldsymbol{r}') = \langle \hat{\psi}_{\bar{\sigma}}^\dagger(\boldsymbol{r}) \hat{\psi}_\sigma^\dagger(\boldsymbol{r}) \hat{\psi}_\sigma^\dagger(\boldsymbol{r}') \hat{\psi}_\sigma(\boldsymbol{r}') \hat{\psi}_\sigma(\boldsymbol{r}) \hat{\psi}_{\bar{\sigma}}(\boldsymbol{r}) \rangle$ is the three-body correlation function which gives the probability of finding three particles with spin $\bar{\sigma}\sigma\sigma$ [40] at locations $\boldsymbol{r}\boldsymbol{r}\boldsymbol{r}'$ respectively. Here $\bar{\sigma}$ refers to the opposite spin of σ. In this way the total loss rate is in units of energy and the microscopic contribution, represented by the prefactor a_s^3 together with the integration over $\boldsymbol{r}'$, is decoupled from the many-body background given by the correlation function. The three-particle correlation function is commonly [35,41,42] treated phenomenologically as $g_{\bar{\sigma}\sigma\sigma}^0(\boldsymbol{r}, \boldsymbol{r}, \boldsymbol{r}') = n_{\bar{\sigma}}(\boldsymbol{r}) n_\sigma(\boldsymbol{r}) n_\sigma(\boldsymbol{r}')$, where the density is assumed to be constant within the integral over $\boldsymbol{r}'$. This form disregards quantum mechanical corrections due to exchange effects and violates the Pauli principle.

(a) Total density

(b) Magnetisation

(c) Recombination rate
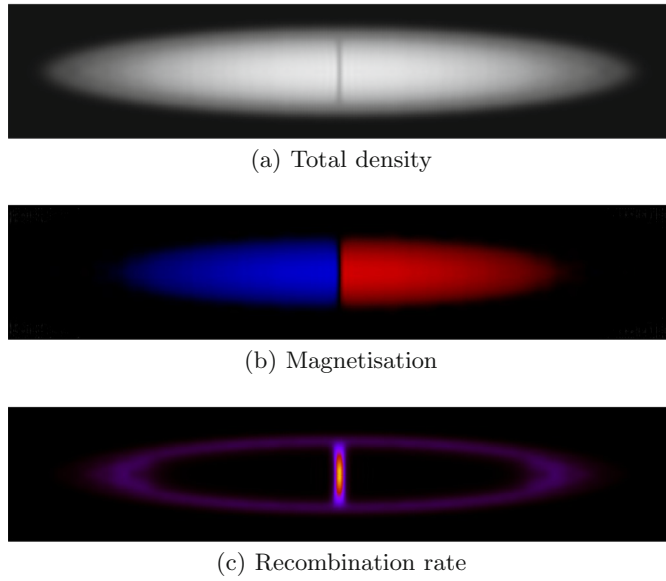
Fig. 3. Total density $n_\uparrow + n_\downarrow$, magnetisation $n_\uparrow - n_\downarrow$ and loss rate Γ in harmonic confinement for the aspect ratio $\lambda = 5$, $k_F^0 a_s \sim 1.4$ and $N_\uparrow = N_\downarrow = 969$. The z and r axes are along the horizontal and vertical directions, respectively.

Within the Kohn-Sham formalism a more accurate representation is

$$g_{\bar{\sigma}\sigma\sigma}(\boldsymbol{r}, \boldsymbol{r}, \boldsymbol{r}') = g^0_{\bar{\sigma}\sigma\sigma}(\boldsymbol{r}, \boldsymbol{r}, \boldsymbol{r}') - n_{\bar{\sigma}}(\boldsymbol{r})|\rho_\sigma(\boldsymbol{r}, \boldsymbol{r}')|^2 \quad (2)$$

where $\rho_\sigma(\boldsymbol{r}, \boldsymbol{r}')$ is the one-body density matrix. The Pauli principle is restored in this formulation as $g_{\bar{\sigma}\sigma\sigma}(\boldsymbol{r}, \boldsymbol{r}, \boldsymbol{r}) \equiv 0$, thus leading to a better estimate of three-body losses.

As molecule formation in the gas is a three-body process and requires both species of fermions to be close to each other, the recombination rate (1) is determined by the total volume where the two spin species are mixed. In a polarised system this amounts to the overlap between ferromagnetic domains at their boundaries, whose structure strongly depends on the external confining potential. To further investigate this effect, we impose a cigar shaped harmonic potential, which has been used in a number of recent experiments [8,13]. With cylindrical symmetry around the z-axis the potential is in the form $V_{HO}(r, z) = 1/2(\omega_r^2 r^2 + \omega_z z^2)$ with aspect ratio $\lambda = \omega_r / \omega_z$. We will consider the spin-balanced case $N_\uparrow = N_\downarrow = N/2$ and normalise the loss rate Γ by the critical recombination rate Γ_c, above which the system is unstable. This value can be estimated from the experimental observation of an equilibrium density distribution up to $k_F a_s \sim 0.4$ for ^{6}Li atoms in an optical dipole trap [13].

With equal number of spin-up and down particles, the ferromagnetic ground state exhibits a domain wall across the middle of the trap, as shown in Figure 3b. Due to repulsion between the two polarized domains there is a drop in total density along this region with a width $\sim 0.5 k_F^{-1}$ (see Fig. 3a), which is, however, below the resolution of current experiments [8]. As shown in Figure 3c, particle loss occurs predominantly at the domain wall in the center of the trap and in the low-density halo on the surface of
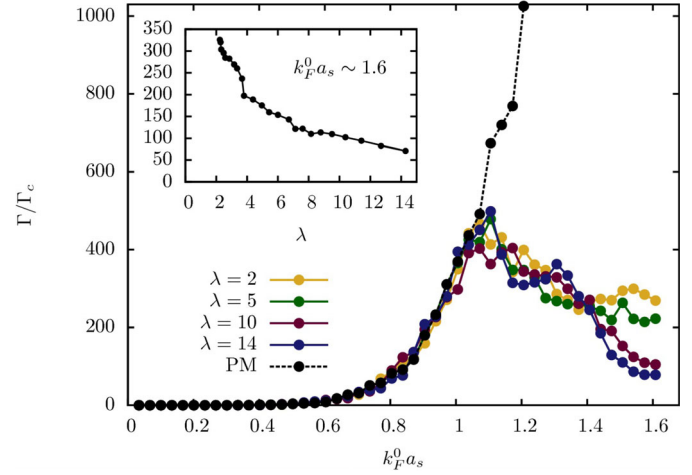

Fig. 4. Normalised recombination rate Γ/Γ_c in harmonic confinement for aspect ratios $\lambda = \{2, 5, 10, 14\}$ and $N_\uparrow = N_\downarrow = 560$ at different interaction strengths. Inset: dependence of Γ/Γ_c on the aspect ratio for $k_F^0 a_s \sim 1.6$. From simulations of different system sizes we checked that the results are not sensitive to the number of atoms in the system.

the clouds where the gas remains unpolarised due to low densities.

One can thus expect that larger aspect ratios may reduce losses due to a smaller area of the domain wall. To investigate this quantitatively we present the results of our calculations for the recombination rate in Figure 4 as a function of interaction strength $k_F a_a$. Starting from a non-interacting gas in the paramagnetic ground state, the recombination rate increases until phase separation due to ferromagnetism sets in and a maximum is reached at $k_F a_s \sim 1.1$, after which total losses are again reduced. A similar dependence of the loss rate on scattering length was observed in the experiment [6] and theoretical studies [42,43]. As the trap is compressed around the z-axis at constant volume $\bar{\omega} = (\omega_r^2 \omega_z)^{1/3}$ and system size N (see inset of Fig. 4), the aspect ratio increases and the recombination rate is indeed significantly reduced. However, with a six times lower recombination rate at $\lambda = 14$ compared to $\lambda = 2$, the loss rate is still above the critical value Γ_c.

We now turn to the most promising way of stabilising the ferromagnetic phase, by reducing the critical scattering length of the ferromagnetic phase transition. This can be achieved by imposing a shallow optical lattice [17], which reduces the kinetic energy loss at the phase transition and thus favors the ferromagnetic state. Figure 5 shows the phase diagram at quarter filling ($\bar{n} = 0.5$) in a shallow 3D cubic optical lattice $V_{\mathrm{OL}}(\boldsymbol{r}) = V_0 \sum_{i=1}^3 \sin^2(\pi \boldsymbol{r}_i / d)$, where V_0 is in units of recoil energy $E_R = \frac{\hbar^2 \pi^2}{2md^2}$ and d is the lattice constant. At quarter filling $\bar{n} = 0.5$, the maximum tolerable $k_F a_s \sim 0.4$ corresponds to $a_s = 0.16d$, which is nearly half the critical scattering length predicted by diffusion Monte Carlo [3,4].

We see that a ferromagnetic phase exists at this scattering length for a lattice depth of about $V_0 \sim 2.5 E_R$. However, the loss rate is likely significantly affected
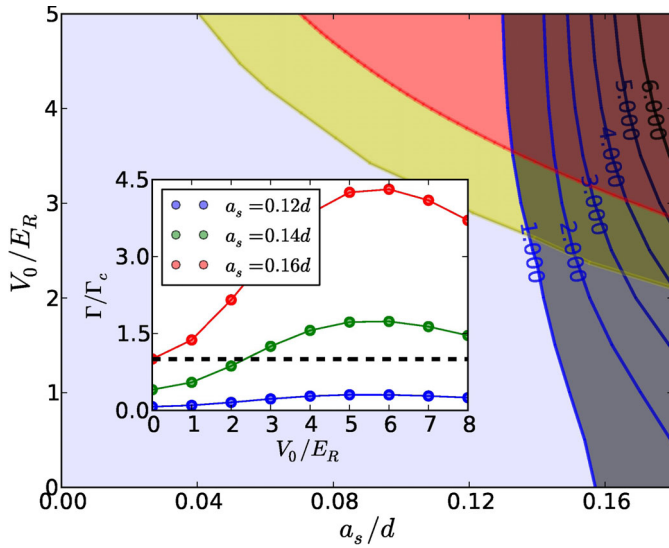
Fig. 5. Contours of constant normalised loss rate Γ/Γ_c at quarter filling $\bar{n} = 0.5$ in an optical lattice. In the shaded region $\Gamma > \Gamma_c$. Red (yellow) region denotes the fully (partially) polarized ferromagnetic phase. Inset: normalised loss rates Γ/Γ_c for $a_s = \{0.12, 0.14, 0.16\}$ at different lattice depths. The dotted line is Γ_c. From simulations at different fillings bellow $\bar{n} = 1.0$, we checked that the physics remains qualitatively the same.

by the presence of a periodic potential. To address this issue we calculate the recombination rate of the paramagnetic state in an optical lattice by integrating over the unit cell equation (1).

The loss rate initially grows as the lattice is ramped up since the density increases at the center of the unit cell (inset of Fig. 5). In very deep lattices the loss rate is reduced when one approaches the regime where the physics is well described by the single band Hubbard model and triple occupation of a lattice site is reduced. In Figure 5 we show contour lines of constant loss rate Γ and indicate by grey shading the regime where we expect three body losses to be above the critical experimental value. We find that despite the increased three-body losses in a shallow lattice, the ferromagnetic phase is stable in a wide region of the phase diagram. Our calculations have not taken into account the quantum Zeno effect [44] which will further suppress three body recombination.

In summary, we have shown that although larger aspect ratios in harmonic confinement can significantly reduce the total recombination rate, the gas remains unstable. However, in an optical lattice the ferromagnetic phase extends down to small enough scattering lengths where three-body recombination is below the critical value. Experimental verification of our results will be solid confirmation of the Stoner model of itinerant ferromagnetism.

References

1. E.C. Stoner, Philos. Mag. Ser. 7 **15**, 1018 (1933)
2. S. Pilati, I. Zintchenko, M. Troyer, Phys. Rev. Lett. **112**, 015301 (2014)
3. S. Pilati, G. Bertaina, S. Giorgini, M. Troyer, Phys. Rev. Lett. **105**, 030405 (2010)
4. S.Y. Chang, M. Randeria, N. Trivedi, Proc. Natl. Acad. Sci. **108**, 51 (2011)
5. S. Giorgini, L.P. Pitaevskii, S. Stringari, Rev. Mod. Phys. **80**, 1215 (2008)
6. G.B. Jo, Y.R. Lee, J.H. Choi, C.A. Christensen, T.H. Kim, J.H. Thywissen, D.E. Pritchard, W. Ketterle, Science **325**, 1521 (2009)
7. H. Zhai, Phys. Rev. A **80**, 051605 (2009)
8. C. Sanner, E.J. Su, W. Huang, A. Keshet, J. Gillen, W. Ketterle, Phys. Rev. Lett. **108**, 240404 (2012)
9. D. Pekker, M. Babadi, R. Sensarma, N. Zinner, L. Pollet, M.W. Zwierlein, E. Demler, Phys. Rev. Lett. **106**, 050402 (2011)
10. C.W. von Keyserlingk, G.J. Conduit, Phys. Rev. B **87**, 184424 (2013)
11. P. Massignan, Z. Yu, G.M. Bruun, Phys. Rev. Lett. **110**, 230401 (2013)
12. E.L. Hazlett, Y. Zhang, R.W. Stites, K.M. O'Hara, Phys. Rev. Lett. **108**, 045304 (2012)
13. Y.R. Lee, M.S. Heo, J.H. Choi, T. Wang, C. Christensen, T. Rvachov, W. Ketterle, Phys. Rev. A **85**, 063615 (2012)
14. C.W. von Keyserlingk, G.J. Conduit, Phys. Rev. A **83**, 053625 (2011)
15. X. Cui, T.L. Ho, Phys. Rev. Lett. **110**, 165302 (2013)
16. C. Kohstall, M. Zaccanti, M. Jag, A. Trenkwalder, P. Massignan, G.M. Bruun, F. Schreck, R. Grimm, Nature **485**, 615 (2012)
17. P.N. Ma, S. Pilati, M. Troyer, X. Dai, Nat. Phys. **8**, 601 (2012)
18. E.H. Lieb, Phys. Rev. Lett. **62**, 1201 (1989)
19. A. Mielke, J. Phys. A **24**, L73 (1991)
20. H. Tasaki, Phys. Rev. Lett. **69**, 1608 (1992)
21. C.C. Chang, S. Zhang, D.M. Ceperley, Phys. Rev. A **82**, 061603 (2010)
22. G. Carleo, S. Moroni, F. Becca, S. Baroni, Phys. Rev. B **83**, 060411 (2011)
23. Y. Nagaoka, Phys. Rev. **147**, 392 (1966)
24. L. Wang, X. Dai, S. Chen, X.C. Xie, Phys. Rev. A **78**, 023603 (2008)
25. P. Hohenberg, W. Kohn, Phys. Rev. B **136**, 864 (1964)
26. W. Kohn, L.J. Sham, Phys. Rev. A **140**, 1133 (1965)
27. A. Bulgac, Y.L. Luo, P. Magierski, K.J. Roche, Y. Yu, Science **332**, 1288 (2011)
28. I. Stetcu, A. Bulgac, P. Magierski, K.J. Roche, Phys. Rev. C **84**, 051309 (2011)
29. N. Helbig, J.I. Fuks, M. Casula, M.J. Verstraete, M.A.L. Marques, I.V. Tokatly, A. Rubio, Phys. Rev. A **83**, 032503 (2011)
30. A. Recati, S. Stringari, Phys. Rev. Lett. **106**, 080402 (2011)

31. M.V. Stoitsov, I.Z. Petkov, Ann. Phys. **184**, 121 (1988)
32. T. Biben, D. Frenkel, J. Phys.: Condens. Matter **14**, 9077 (2002)
33. N.D. Mermin, Phys. Rev. A **137**, 1441 (1965)
34. U. Gupta, A. Rajagopal, Phys. Rep. **87**, 259 (1982)
35. R.A. Duine, A.H. MacDonald, Phys. Rev. Lett. **95**, 230403 (2005)
36. H. Heiselberg, Phys. Rev. A **83**, 053635 (2011)
37. G.J. Conduit, B.D. Simons, Phys. Rev. Lett. **103**, 200403 (2009)
38. E. Runge, E.K.U. Gross, Phys. Rev. Lett. **52**, 997 (1984)
39. D. Petrov, Phys. Rev. A **67**, 010703 (2003)
40. P.O. Fedichev, M.W. Reynolds, G.V. Shlyapnikov, Phys. Rev. Lett. **77**, 2921 (1996)
41. G. Conduit, E. Altman, Phys. Rev. A **83**, 043618 (2011)
42. L.J. LeBlanc, J.H. Thywissen, A.A. Burkov, A. Paramekanti, Phys. Rev. A **80**, 013607 (2009)
43. S. Zhang, T.L. Ho, New J. Phys. **13**, 055003 (2011)
44. M.C. Fischer, B. Gutiérrez-Medina, M.G. Raizen, Phys. Rev. Lett. **87**, 040402 (2001)